JOURNAL OF COMPUTATIONAL PHYSICS 59, 152–166 (1985)

An Analysis of a Finite-Difference and a Galerkin Technique Applied to the Simulation of Advection and Diffusion of Air Pollutants from a Line Source

E. RUNCA

Technital S.p.A., Via Carlo Cattaneo, 20, I-37121 Verona, Italy

P. MELLI

IBM *Scientific Center, Via del Giorgione 129, I-00147 Rome, Italy*

AND

F. SARDEI

Max Planck Institut für Plasmaphysik, D-8046 Garching bei München, Munich, Federal Republic of Germany

Received April 7, 1982; revised July 16, 1984

A finite-difference scheme and a Galerkin scheme are compared with respect to a very accurate solution describing time-dependent advection and diffusion of air pollutants from a line source in an atmosphere vertically stratified and limited by an inversion layer. The accurate solution was achieved by applying the finite-difference scheme on a very refined grid with a very small time step. The grid size and time step were defined according to stability and accuracy criteria discussed in the text. It is found that for the problem considered the two methods can be considered equally accurate. However, the Galerkin method gives a better approximation in the vicinity of the source. This was assumed to be partly due to the different way the source term is taken into account in the two methods. Improvement of the accuracy of the finite-difference scheme was achieved by approximating, at every step, the contribution of the source term by a Gaussian puff moving and diffusing with the velocity and diffusivity of the source location, instead of utilizing a stepwise function for the numerical approximation of the δ function representing the source term.

INTRODUCTION

Simulation of advection and diffusion of pollutants in environmental media are required for defining both planning and control strategies. In many situations, the problem is the dispersion of pollutants from a point source in a turbulent flow. A

0021-9991/85 $3.00

classical mathematical model of this process is provided by the equation of mass conservation, which, neglecting removal processes, takes the form

$$\frac{\partial C}{\partial t} + \nabla \cdot (\mathbf{U}C) = \nabla \cdot (\bar{\bar{K}} \cdot \nabla C) + Q\delta(\mathbf{x} - \mathbf{x}_s). \tag{1}$$

In (1), C is the mean (ensemble average) concentration of the pollutant considered, $\mathbf{U}$ is the mean flow velocity vector, $\bar{\bar{K}}$ is the turbulent diffusivity tensor, Q is the emission rate of the point source located at (x_s, y_s, z_s), and $\delta(\cdot)$ is Dirac's function.

Equation (1) is based on the mixing length or gradient transport hypothesis [5], which, by analogy with molecular diffusion, assumes that the turbulent flux can be expressed as the product of an eddy diffusivity coefficient and the gradient of the mean concentration. The gradient transfer hypothesis implies that Eq. (1) can only resolve spatial and temporal variations of the concentration on scales larger than the respective Lagrangian scales of the turbulence.

Limitations of the gradient transfer hypotheses are discussed by Corrsin [2], Lamb and Seinfeld [4], and other researchers. The present study is concerned with the problem of solving Eq. (1) by numerical methods. Both a finite-difference and a Galerkin scheme have been used to simulate numerically the processes described by Eq. (1). The schemes considered are compared with respect to their application to the classical two-dimensional problem of dispersion of air pollutants from an elevated line source in the atmospheric boundary layer. For this specific problem, the finite-difference scheme is used to compute a very accurate solution by solving Eq. (1) on a highly refined grid and using an extremely small integration time step. This solution is considered to be a high-quality approximation of the exact solution in the sense that further refinement of the grid and of the time step left the results unchanged on the scale of accuracy discussed in this study. The finite difference and the Galerkin schemes are then applied to solve the same problem on coarse grids and with large time steps; the results are then compared with the refined solution. Finally, an improved method of treating the source term of Eq. (1) when finite different schemes are applied is discussed.

Mathematical Model

The numerical schemes in this study were applied to a problem which can be considered to be a mathematical description of the dispersion of an inert air pollutant from a crosswind line source of infinite extent and uniform emission in an atmosphere vertically limited by an inversion layer. The x axis is taken along the wind vector (assumed to have components only in the horizontal plane) and the y dependence of the problem is neglected. If it is also assumed that the axes of the frame of reference chosen are the principal axes of the diffusivity tensor and that

ground and inversion layers completely reflect the diffusing material, the problem can be formulated as follows:

$$\frac{\partial C}{\partial t} + U(z)\frac{\partial C}{\partial x} = K_x \frac{\partial^2 C}{\partial x^2} + \frac{\partial}{\partial z}\left(K_z \frac{\partial C}{\partial z}\right) + Q\,\delta(z - z_s)\,\delta(x - x_s); \tag{2}$$

$$K_z \frac{\partial C}{\partial z} = 0, \qquad z = 0, H, \tag{2a}$$

$$C(x, z, t) = 0, \qquad x = \pm\infty, \tag{2b}$$

$$C(x, z, t) = 0, \qquad t = 0, \tag{2c}$$

where H is the height of the inversion layer. Equation (2) is derived from Eq. (1) with the additional assumptions of constant horizontal diffusivity and wind and vertical diffusivity as functions only of the vertical coordinate.

To generalize results given by the numerical solution to Eq. (2) and related boundary and initial conditions of Eqs. (2a)–(2c), the variables and parameters x, z, t, U, K_x, K_z, C have been expressed in units of $H^2U(H)/K_z(H)$, H, $H^2/K_z(H)$, $U(H)$, $H^2U^2(H)/K_z(H)$, $K_z(H)$, and $Q/U(H)\,H$, respectively. Use of these normalizing factors leaves Eqs. (2)–(2c) formally unchanged except for the emission rate and the inversion layer height, which are both normalized to unity.

Finite-Difference Scheme

The finite-difference scheme used is based on the method of fractional steps (see, for example, [18], and, for application to problems similar to the one discussed here [16, 12, 13]. According to this procedure, Eq. (2) is split into the following sequence of one-dimensional, normalized equations:

$$\frac{\partial C}{\partial t} = \delta(x - x_s)\,\delta(z - z_s), \tag{3a}$$

$$\frac{\partial C}{\partial t} = -U\frac{\partial C}{\partial x}; \qquad C(x, z, t) = 0, \quad x = \pm\infty, \tag{3b}$$

$$\frac{\partial C}{\partial t} = K_x \frac{\partial^2 C}{\partial x^2}; \qquad C(x, z, t) = 0, \quad x = \pm\infty, \tag{3c}$$

$$\frac{\partial C}{\partial t} = \frac{\partial}{\partial z}\left(K_z \frac{\partial C}{\partial z}\right); \qquad K_z \frac{\partial C}{\partial z} = 0, \quad z = 0, 1. \tag{3d}$$

At each time step, the above equations are solved sequentially by taking as initial concentration the one obtained by solving the previous equation. Each of the above equations is numerically integrated over the time step Δt. The concentration field

obtained after integration to Eq. (3d) provides the initial condition to Eq. (3a) for the next time step. In practice, the processes described by Eqs. (3a)–(3d) are considered to be separate occurrences at each time step.

The source step is calculated by assigning a weighted distribution of the released material to the grid points surrounding the source at each time step. For advection and diffusion steps two simple, mass-conserving, second-order schemes are chosen, namely the one-step Lax-Wendroff and the standard Cranck-Nicolson schemes [9], respectively;

$$C_{ik}^{*} = C_{ik}^{n} + \gamma_{ik}\, \Delta t/\Delta x\, \Delta z, \tag{4a}$$

$$C_{ik}^{**} = C_{ik}^{*} + \left[-\Delta t\, U \frac{\delta}{\delta x} + \frac{\Delta t^2 U^2}{2} \frac{\delta^2}{\delta x^2} \right] C_{ik}^{*}, \tag{4b}$$

$$C_{ik}^{***} = C_{ik}^{**} + \left[\Delta t\, K_x \frac{\delta^2}{\delta x^2} \right] \left(\frac{C_{ik}^{***} + C_{ik}^{**}}{2} \right), \tag{4c}$$

$$C_{ik}^{n+1} = C_{ik}^{***} + \left[\Delta t \frac{\delta}{\delta z} \left(K_z \frac{\delta}{\delta z} \right) \right] \left(\frac{C_{ik}^{n+1} + C_{ik}^{***}}{2} \right), \tag{4d}$$

where $\gamma_{ik} \leqslant 1$ is a weighting factor depending on the position of the source with respect to the grid and $\delta/\delta x$, $\delta^2/\delta x^2$, $\delta/\delta z (\cdot \delta/\delta z)$ are the standard second order centered spatial difference operators. $\sum \gamma_{ik} = 1$ is, of course, required to ensure consistency. Since strong spatial variations are only expected to occur in a narrow region close to the source location, higher than second-order advection schemes

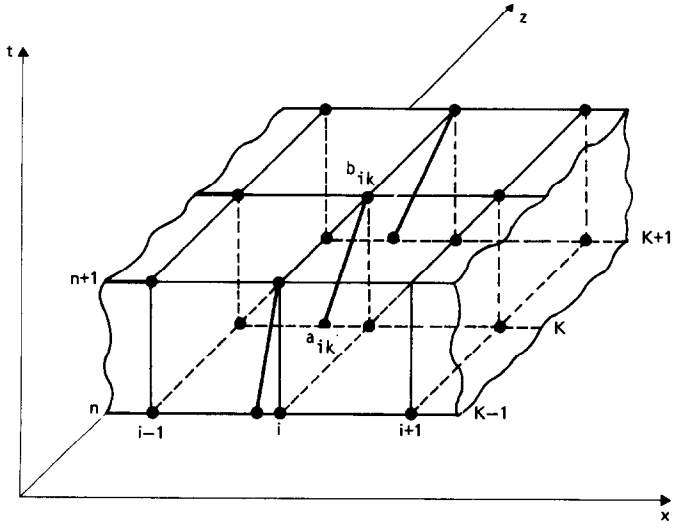

FIG. 1. Geometric description of the finite-difference scheme. *ab* is the trajectory of the pollutant particle at level z_k.

(see, for example, [1, 6]) would only give significantly better results in this region, at least on the moderate level accuracy involved in this study. To compensate these errors as well as those arising from Eq. (4a) without losing the advantages of the Lax–Wendroff scheme in terms of simplicity and efficiency (e.g., full vectorization capability), an improved solution technique for the vicinity of the source is proposed (see below).

A physical interpretation of the given splitting procedure can be illustrated as follows:

The r.h.s. of Eq. (4b) can be interpreted as a second-order spatial interpolation of the concentration at the old time level at the position a_{ik}, which is located on the same characteristic as the point b_{ik} at the new time level (see Fig. 1). From Eqs. (4b)–(4d) it follows that, outside the source location, the new concentration field C_{ik}^{n+1} only depends on the old concentration field $C_{a_{ik}}$ defined along the same characteristics. That is, owing to the fractional step technique and the explicit treatment of the advection step, the algorithm simulates the diffusion process following the trajectories of the advected fluid elements, i.e., in a way close to the physical nature of the advective motion [14].

Galerkin Scheme

The Galerkin scheme employed in this study is programmed on the same grid geometry used for the finite-difference scheme. A Galerkin scheme similar to the one discussed here has been applied by Melli [7].

The elements of the rectangular grid representing the integration domain are divided into triangles by means of diagonals. On the triangular elements thus obtained the set of linear isoparametric functions ϕ is defined. The concentration is expressed as a linear combination of this set of functions,

$$C \simeq \sum_{j=1}^{N} C_j \phi_j, \tag{5}$$

where N is the total number of grid points used and C_j is the value of the concentration at the grid points.

By substitution of Eq. (5) in Eq. (2) and application of the Galerkin principle [8], the following system of ordinary differential equations is obtained,

$$\begin{aligned}
&\sum_{j=1}^{N}\left[\iint_{\Omega}\phi_i\phi_j\,dx\,dz\right]\frac{dC_j}{dt}+\sum_{j=1}^{N}\left[\iint_{\Omega}U\phi_i\frac{\partial\phi_j}{\partial x}\,dx\,dz\right]C_j\\
&\quad+\sum_{j=1}^{N}\left[\iint_{\Omega}K_x\frac{\partial\phi_i}{\partial x}\frac{\partial\phi_j}{\partial z}\,dx\,dz+\iint_{\Omega}K_z\frac{\partial\phi_i}{\partial z}\frac{\partial\phi_j}{\partial z}\,dx\,dz\right]C_j\\
&\quad+\sum_{j=1}^{N}\left[\int_{\Gamma}K_x\phi_i\frac{\partial\phi_j}{\partial x}\cos\widehat{xn}\,ds\right]C_j=\phi_i(x_s,h_s);\qquad i=1,2,\ldots,N,
\end{aligned}\tag{6}$$

where Ω is the region of integration, Γ its boundary, s the curvilinear coordinate along Γ, and n the inward unit vector normal to Γ. It must be noted that boundary conditions of Eq. (2a) have already been used in deriving Eq. (6), leading to cancellation of integrals along Γ containing vertical diffusion terms. The integrals

$$\int_{\Gamma} K_x \phi_i \frac{\partial \phi_j}{\partial x} \cos \widehat{xn}\, ds$$

are computed in accordance with the assumption that concentration vanishes on lateral boundaries (the same assumption as used for the finite-difference scheme).

Discretization of the time derivative by means of the Crank–Nicolson scheme leads to a system of linear algebraic equations which is solved by means of the Seidel iterative technique [3].

Stability and Accuracy

The application of Von Neuman's stability analysis to the fractional step procedure presented shows that the amplification factor of a Fourier concentration component is the product of the amplification factors of the single steps [10]. The stability condition required by the scheme is therefore only the Courant condition

$$\frac{U \Delta t}{\Delta x} < 1. \tag{7}$$

This stems from the use of Lax–Wendroff scheme for the advection step.

The computational dissipation associated with the Lax–Wendroff scheme is of higher order than $K_c \partial^2 C/\partial x^2$ [6], where K_c is the generalized computational diffusion coefficient and the dispersion error is of third order in Δx [10].

No additional stability limitations are introduced by the diffusion steps (4c), (4d) since the Crank–Nicolson scheme is unconditionally stable. However, to avoid negative overshooting of the high-order Fourier components the following restrictions on Δt are also imposed for reasons of accuracy:

$$\frac{K_x \Delta t}{\Delta x^2} < \frac{1}{2}, \tag{8}$$

$$\frac{K_z \Delta t}{\Delta z^2} < \frac{1}{2}. \tag{9}$$

The Galerkin scheme is unconditionally stable, the amplification factor being equal to one for any wave component.

Refined Solution

Equations (2)–(2c) are solved with the above-defined finite-difference scheme for (in normalized units)

$$K_x = 10^{-4},$$
$$K_z = ze^{-4(z-1)},$$
$$U = z^{0.2},$$

over the region $0 \leqslant x \leqslant 2.4 \times 10^{-2}$ and $0 \leqslant z \leqslant 1$.

To avoid errors arising from the imposed vanishing concentrations at the upwind and downwind boundaries, the analysis of the results is restricted to a subdomain smaller than the integration domain (see below). Experiments with larger integration domain than the one chosen did not significantly change the concentraion field in the subdomain.

The vertical eddy diffusivity chosen is the same as that adopted by Shir and Shieh [16]; it can be considered representative of diffusion in a neutral atmosphere [15, 17, 11].

The integration region was described by 481 points in the horizontal axis and 97 in the vertical axis, corresponding to $\Delta x = 5 \times 10^{-5}$ and $\Delta z \simeq 1.04 \times 10^{-2}$, respectively. With $\Delta t = 1.25 \times 10^{-5}$, the following values are obtained for Eqs. (7)–(9),

$$\frac{U_{\max} \Delta t}{\Delta x} = 0.25,$$
$$\frac{K_x \Delta t}{\Delta x^2} = 0.5,$$
$$\frac{K_{z_{\max}} \Delta t}{\Delta z_2} \cong 0.58.$$

With the above parameters and grid geometry, the integration is carried out for 3072 time steps for two different source heights $z_s = 0.25$ and $z_s = 0.5$ and horizontal position $x_s = 38 \times 10^{-4}$. After this time, steady-state conditions are approximately established.

Results

In this section, the solutions computed by te Galerkin and finite-difference schemes on coarser grids with larger time steps are compared with the one discussed in the section entitled Refined Solution. This comparison is carried out in terms of root-mean-square deviations of the solutions given by the two schemes

from the refined solution. Specifically, the following normalized value of the root mean square of the deviations is used:

$$\varepsilon_{\text{mean}(t)} = \frac{\left\{\frac{1}{A}\iint_R [C(x, z, t) - C_{\text{ref}}(x, z, t)]^2 \, dx \, dz\right\}^{1/2}}{\frac{1}{A}\iint_R C_{\text{ref}}(x, z, t) \, dx \, dz}. \tag{10}$$

Here A is the area of the already mentioned subdomain R of the integration region defined by $0.32 \times 10^{-2} \leqslant x \leqslant 2.24 \times 10^{-2}$, $0 \leqslant z \leqslant 1$.

Note that the root mean square of the deviations is normalized, at a given time, to the mean concentration of the refined solution to obtain error estimates accounting for the increasing quantity of the pollutant emitted in the region considered.

Figure 2 depicts the normalized root mean square of the deviations defined by Eq. (10) for the source located at $z_s = 0.5$. It shows the behaviour with increasing time of the normalized root mean square of the deviations for both the finite-difference (solid lines) and Galerkin schemes (dashed lines).

For 61×13 grid points the Galerkin method is clearly more accurate than the finite-difference algorithm. This is essentially due to the higher discretization quality inherent in the scheme. This superiority is, however, reduced if coarser grids are used. If the source height is changed to $z_s = 0.25$, the two schemes are nearly equivalent, as shown in Fig. 3.

Both Figs. 2 and 3 show that $\varepsilon_{\text{mean}}$ decreases with time, which indicates a decreasing level of errors in the downwind direction. This is not surprising since the gradients of the concentration become smaller as the pollutant front moves away

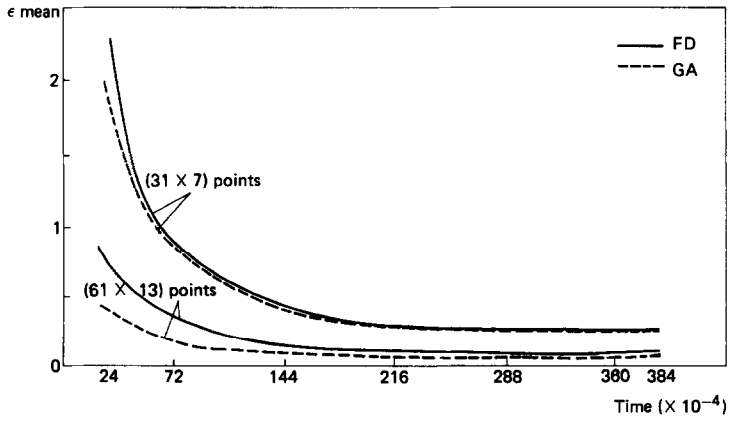

FIG. 2. Time evolution of $\varepsilon_{\text{mean}}$ for the finite-difference and Galerkin schemes for grids of (31×7) points and (61×13) points. In both cases, the time step was taken equal to Δx. Source height $= 0.5$.

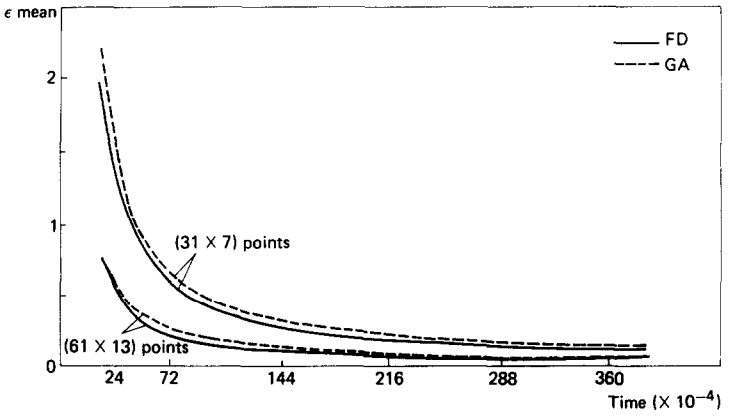

FIG. 3. Same as Fig. 2, except that $z_s = 0.25$.

from the source. The situation is clearly depicted in Fig. 4, which displays the isolines of the percentage error

$$\varepsilon_p = |C - C_{\text{ref}}| \times 100/C_{\text{ref}}$$

for the source located at $z_s = 0.25$ and a grid of 61×13 points.

The isolines of Fig. 4 indicate that the area of small errors increases with increasing simulation time. The Galerkin method shows areas of small errors wider than the ones given by the finite-difference scheme. However, it also presents wider areas of larger errors close to the boundaries of the integration region. This explains the results of Fig. 3 and the reverse situation with respect to Fig. 2. Reducing the source height increases the error induced by the boundaries of the region in the Galerkin method.

The results of Fig. 2–4 show that for large physical simulation times a reasonable approximation of the solution can be achieved with a limited number of points and a large time step. To guarantee a sufficiently accurate solution for a small simulation time, especially at points far from the source, the number of grid points must be increased and the time step shortened. It appears from the results presented that to avoid errors not much larger than 10% at ground level, the number of grid points should be of the order of 61×13 and the time step should be chosen in accordance with the stabilitity and accuracy requirements stated above. In reality, this is the level of discretization used in applications reported in the literature [16] and [13].

Analysis of Fig. 4 also indicates that the Galerkin method is superior to the finite-difference scheme in approximating the concentration field in the region close to the source, where the maximum concentration gradients occur. This is because the discontinuity introduced by the source term is somewhat smoothed out by the Galerkin method through the integration process leading to Eq. (6). In the finite-

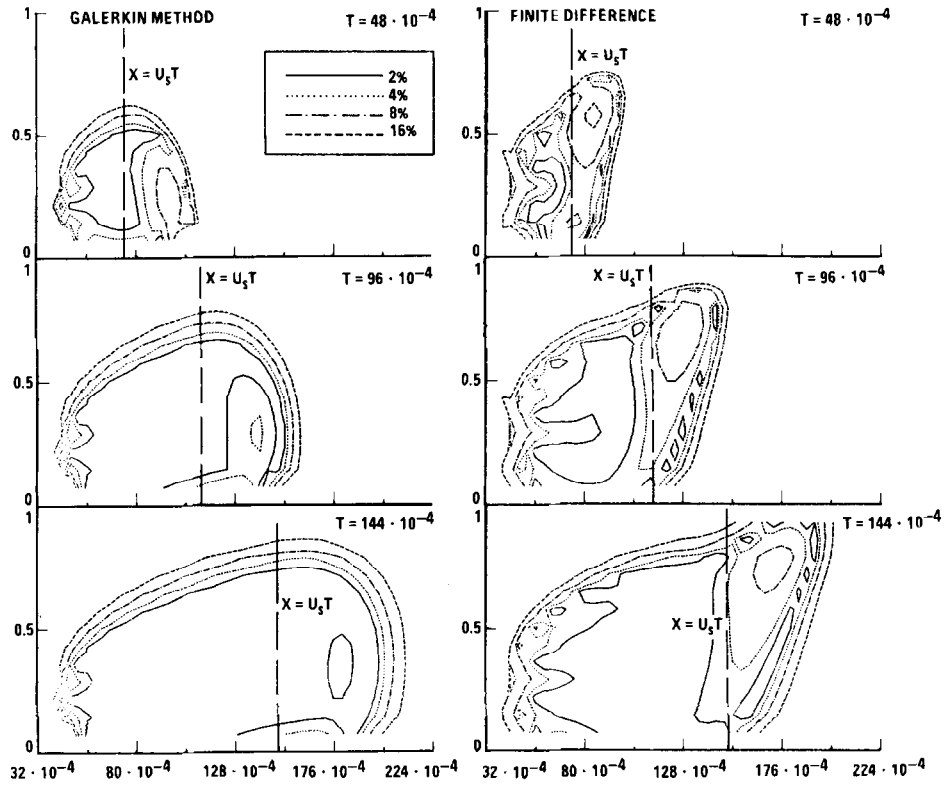

FIG. 4. Time sequences of percentage error distribution for $z_s = 0.25$. U_s is the wind speed at source height.

difference scheme, the source term is treated "empirically" by adding a contribution to the concentration in the points of the grid close to the source in such a way that at every time step the quantity Δt is injected in the region. This approach introduces large errors close to the source which, by virtue of the diffusion operator, are damped downwind from the source. Figure 4 finally shows that the finite-difference method seems to be producing small wave packets of small concentration errors in the regions with high gradients or high time variation rates of the concentration. Using a filtering algorithm would probably eliminate them, thus improving the optics of Fig. 4. However, it would not change any of the discussed results, since these errors practically do not exceed the 2% level, and also they affect only very narrow regions of the domain.

On the basis of the results shown, the Galerkin method can be considered slightly superior to the finite-difference algorithm as far as accuracy is concerned. On the other hand, it requires more computational effort. In fact, it requires the solution of a seven-diagonal system equal in dimension to the total number of grid points

$M \times N$, whereas the finite-difference method requires the solution of M tridiagonal systems of dimension N and N tridiagonal systems of dimension M.

To reduce the errors of the finite-difference algorithm close to the source, an improved method of solution is discussed next.

Source Term Approximation

Owing to the linearity of Eq. (1), the diffusion process from a point source can be seen at time $n\,\Delta t$ as the result of two processes. One is the diffusion process of the concentration field C, the other the diffusion process of the amount of pollutant $\int_{(n-1)\,\Delta t}^{n\,\Delta t} Q(t')\,dt'$ released by the source in the time interval Δt.

The above consideration suggests treating the problem as follows. For simplicity, let us examine the one-dimensional case with time-varying emission rate:

$$\frac{\partial C}{\partial t} = -U\frac{\partial C}{\partial x} + K_x\frac{\partial^2 C}{\partial x^2} + Q(t)\,\delta(x_s - x). \tag{11}$$

The concentration at the new time level C^{n+1} is approximated by the sum of two contributions C'^{n+1} and C''^{n+1} resulting from the solution of the same transport equation, but with two different initial conditions,

$$\frac{\partial C'}{\partial t} = -U\frac{\partial C'}{\partial x} + K_x\frac{\partial^2 C'}{\partial x^2}; \qquad C'^n = C^n, \tag{12}$$

$$\frac{\partial C''}{\partial t} = -U\frac{\partial C''}{\partial x} + K_x\frac{\partial^2 C''}{\partial x^2}; \qquad C''^n = Q^{n+1/2}\,\Delta t\,\delta(x - x_s), \tag{13}$$

$$C^{n+1}_{\text{appr}} = C'^{n+1} + C''^{n+1}. \tag{14}$$

The intrinsic error associated with the superposition approximation can be shown to be of first order in Δt (see Appendix).

Reduction to second order can be obtained if Eq. (13) is integrated over half a time step (see Appendix). However, numerical tests showed empirically that the results are more accurate if the same time interval Δt is chosen for both Eqs. (12) and (13). The reason for this behaviour is not clear to the authors. It may be related to the singularity at the source location, where the δ-function produces a discontinuous derivative of the concentration. This discontinuity may be approximated more accurately if the material $Q\,\Delta t$, injected at any time step, is numerically advected over the full distance $U\,\Delta t$ corresponding to its physical travel path.

Since the initial values for Eq. (13) are independent of C, this equation need only be solved for one time step. In fact, the same normalized concentration field $C''^{n+1}/Q^{n+1/2}$ is obtained for any n, provided U and K_x are time-independent or vary in a time scale larger than that of the described transport process. Further-

more, one can use for Eq. (13) a finer grid than for Eq. (12) and integrate over m smaller time steps Δt_s, where $\Delta t_s = \Delta t/m$. Finally, Eq. (13) can be solved by a different numerical or analytical method, which is more suited to treating a discontinuous source term. Owing to the superposition property, these arguments are, of course, valid for multiple source configurations as well.

If wind velocity and diffusivity are approximated by their values at the source location and finite boundary effects are neglected,[1] Eq. (13) has a standard Gauss solution, which, for a general $3D$ case, reads

$$C''^{n+1} = \frac{Q^{n+1/2}\,\Delta t}{8(\pi\,\Delta t)^{3/2}(K_{x_s}K_{y_s}K_{z_s})^{1/2}} \exp\left\{ -\frac{(x - U_s\,\Delta t - x_s)^2}{4K_{x_s}\,\Delta t} - \frac{(y - V_s\,\Delta t - y_s)^2}{4K_{y_s}\,\Delta t} - \frac{(z - W_s\,\Delta t - z_s)^2}{4K_{z_s}\,\Delta t} \right\}. \tag{15}$$

Values given by Eq. (15) must be normalized to guarantee that at every time step the amount $\int_{(n-1)\,\Delta t}^{n\,\Delta t} Q(t')\,dt'$ is injected into the region.

Results from the application of the above algorithm are shown in Fig. 5 and 6, which compare the root mean square of the deviations given by the finite-difference scheme as applied in Fig. 2 and 3 with that obtained by treating the source term as illustrated above. Figures 5 and 6 refer to a grid of 31×7 points and to a source located at $z_s = 0.5$ and 0.25, respectively. The reduction of $\varepsilon_{\text{mean}}$ is greater for short simulation times and becomes negligible for long simulation times, thus confirming

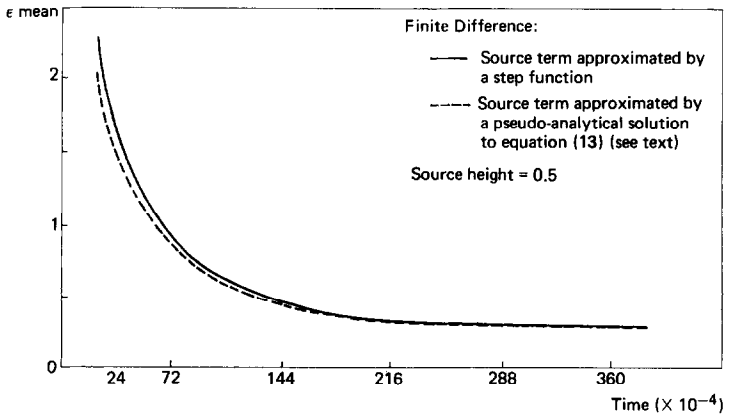

FIG. 5. Comparison of $\varepsilon_{\text{mean}}$ given by the finite difference (solid line) for a grid of (31×7) points and source height = 0.5 (same as in Fig. 2) with the $\varepsilon_{\text{mean}}$ achieved by treating the source term as proposed in the text (broken line).

[1] Equation (15) can be modified easily to account for reflective boundaries.

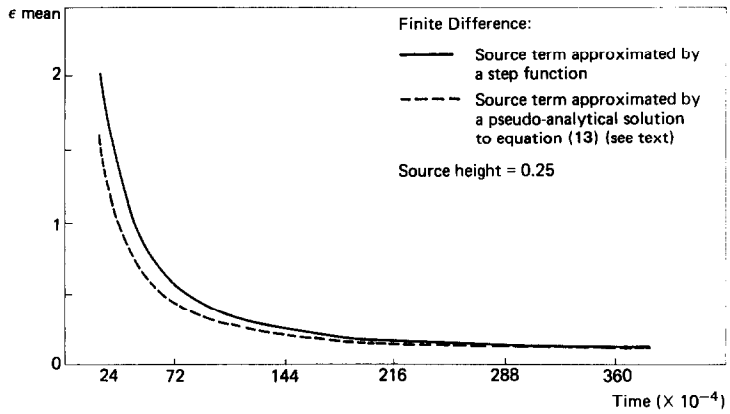

FIG. 6. Same as for Fig. 5, except that $z_s = 0.25$.

that errors in the treatment of the source term are computationally damped by the diffusion operator downwind from the source.

Errors introduced by approximating wind velocity and diffusivity by their values at the source location could be reduced by using more accurate solutions than the one given by Eq. (15). Since improvement of the accuracy is primarily to be expected close to the source, the suggested algorithm should be particularly efficient in multiple-source problems.

CONCLUSION

A finite-difference and a Galerkin scheme are used to solve numerically a boundary value problem describing advection and diffusion of air pollutants from an elevated line source in an atmosphere vertically limited by an inversion layer.

Comparison of the results given by the two schemes with a very accurate solution indicates that for both methods the grid spacing and integration time step ought not to exceed the limits discussed in the text to ensure a sufficiently accurate numerical solution, i.e., to avoid a percentage error much larger than 10% for significant values of the solution. Within this moderate level of overall accuracy, application of the two methods to the problem discussed in this paper give nearly equivalent results.

The Galerkin method, however, is better than the finite-difference scheme at describing the region close to the source for short simulation times. The two schemes prove equivalent for simulation times approaching the steady state.

The errors presented by the finite-difference scheme in points close to the source can be ascribed to the inaccurate estimation of the contribution given at every time step by the source term. By improving such an estimation deviation of the finite-dif-

ference solution from the accurate one could be reduced. The proposed treatment of the source term by increasing the accuracy of the solution close to the source appears relevant to multiple source situations.

APPENDIX

Taylor's expansion of C in Δt and substitution of C_t, C_{tt} from Eq. (11) and its time derivative yield for the concentration at the new time level:

$$C^{n+1} = \left[1 + \Delta t\left(-U\frac{\partial}{\partial x} + K_x\frac{\partial^2}{\partial x^2}\right) + \frac{\Delta t^2}{2}\left(-U\frac{\partial}{\partial x} + K_x\frac{\partial^2}{\partial x^2}\right)^2\right] C^n + \Delta t\left[1 + \frac{\Delta t}{2}\left(-U\frac{\partial}{\partial x} + K_x\frac{\partial^2}{\partial x^2} + \frac{\partial}{\partial t}\right)\right] Q^n\,\delta(x - x_s) + O(\Delta t^3) \quad \text{(A1)}$$

The corresponding expressions for C'^{n+1}, C''^{n+1}, derived by using Eqs. (12), (13), read

$$C'^{n+1} = \left[1 + \Delta t'\left(-U\frac{\partial}{\partial x} + K_x\frac{\partial^2}{\partial x^2}\right) + \frac{\Delta t'^2}{2}\left(-U\frac{\partial}{\partial x} + K_x\frac{\partial^2}{\partial x^2}\right)^2\right] C'^n + O(\Delta t'^3) \quad \text{(A2)}$$

$$C''^{n+1} = \Delta t\left[1 + \Delta t''\left(-U\frac{\partial}{\partial x} + K_x\frac{\partial^2}{\partial x^2}\right) + \frac{\Delta t}{2}\frac{\partial}{\partial t}\right] Q^n\,\delta(x - x_s) + O(\Delta t''\,\Delta t^2) \quad \text{(A3)}$$

where the expansion

$$Q^{n+1/2} = \left[1 + \frac{\Delta t}{2}\frac{\partial}{\partial t}\right] Q^n + O(\Delta t^2) \quad \text{(A4)}$$

has been used. Comparison of the exact solution C^{n+1} to the solution obtained by superposition $C'^{n+1} + C''^{n+1}$ gives

$$\frac{|C^{n+1} - (C'^{n+1} + C''^{n+1})|}{\Delta t} = O(\Delta t) \qquad \text{for} \begin{cases} \Delta t' = \Delta t, \\ \Delta t'' = \Delta t, \end{cases} \quad \text{(A5)}$$

$$\frac{|C^{n+1} - (C'^{n+1} + C''^{n+1})|}{\Delta t} = O(\Delta t^2) \qquad \text{for} \begin{cases} \Delta t' = \Delta t, \\ \Delta t'' = \Delta t/2. \end{cases} \quad \text{(A6)}$$

These expressions show that first or second order accuracy is obtained by integrating Eq. (13) over a full or half time step, respectively.

REFERENCES

1. R. BERKOWICZ AND L. P. PRAHM, *J. Appl. Meteorol.* **18** (1979), 266.
2. S. CORRSIN, "Advances in Geophysics," Vol. 18A, pp. 25–60, Academic Press, New York, 1974.
3. C. E. FROBERG, "Introduction to Numerical Analysis," Addison–Wesley, London, 1966.
4. R. G. LAMB AND J. H. SEINFELD, *Environm. Sci. Technol.* **7** (1973), 253.
5. D. C. LESLIE, "Development in the Theory of Turbulence," Oxford Univ. Press (Clarendon), London, 1973.
6. P. E. LONG, JR. AND D. W. PEPPER, *J. Appl. Meteorol.* **20** (2) (1981), 146.
7. P. MELLI, An application of the Galerkin method to the Eulerian–Lagrangian treatment of time dependent advection and diffusion of air pollutants, *in* "Proceedings, International Conference Finite Elements for Water Resources (Princeton)," Pentech Press, Plymouth, England, 1976.
8. A. R. MITCHELL AND R. WAIT, "The Finite Element Method in Partial Differential Equations," Wiley, New York, 1977.
9. R. D. RICHTMYER AND K. W. MORTON, "Different Methods for Initial-Value Problems," Wiley–Interscience, New York, 1967.
10. J. R. ROACHE, "Computational Fluid Dynamics," Hermosa, Albuquerque, N. M., 1972.
11. A. G. ROBINS, *Atmos. Environ.* **12** (1978), 1021.
12. E. RUNCA AND F. SARDEI, *Atmos. Environ.* **9** (1975), 69.
13. E. RUNCA, P. MELLI, AND A. SPIRITO, "Real Time Forecasting of Air Pollution Episode in the Venetian Region," IIASA Res. Rep. RR-79-11, International Institute for Applied Systems Analysis, Laxenburg, Austria, 1979.
14. F. SARDEI AND E. RUNCA, An efficient numerical scheme for solving time dependent problems of air pollution advection and diffusion *in*, "Proceedings, IBM Seminar on Air Pollution Modelling," IBM Italy Tech. Rep., Rome, Italy, 1975.
15. C. C. SHIR, *J. Atmos., Sci.* **30** (1973), 1327.
16. C. C. SHIR AND L.H. SHIEH, *J. Appl. Meteorol.* **13**, (1974) 185.
17. J. C. WYNGAARD, O. R. COTE, AND K. S. RAO, Modeling the atmospheric boundary layer, *in* "Advances in Geophysics," 1974.
18. N. N. YANENKO, "The Method of Fractional Steps," Springer, Berlin, 1971.